RGD peptide functionalized graphene oxide: a bioactive surface for cell-material interactions

C. H. Zhao[a,*,#], X. P. Zhang[b,#], L. Zhang[c]
[a]*School of Medicine, Hubei Polytechnic University, Huangshi 435003, China*
[b]*Division of Academic Research, Tongren Polytechnic College, Tongren 554300, China*
[c]*Department of Pharmacy,Changhai Hospital, Naval Medical University, Shanghai 200433, China*

Recently, functionalized graphene-based nanomaterials have gained tremendous attention in biomedical field owing to their biocompatibility, surface functionalizability and their unique mechanical, electronic, and optical properties. Herein, we report a facile one step modification of graphene oxide by RGD peptide, which is known to improve the tissue–material contact by highly specific binding to cellular membrane receptors known as integrins. A detailed structural and morphological characterization of the obtained RGD functionalized graphene oxide (GO-RGD) was performed. The synthesized bioactive composite was used to prepare RGD-GO films by a vacuum filtration method. Additionally, mouse osteoblastic cell (MC3T3-E1) functions including cell attachment, adhesion, proliferation, and differentiation were investigated on GO-RGD films. The results indicated that MC3T3-E1 cell functions were significantly enhanced on GO-RGD films comparing with GO films without functionalization. This study not only demonstrates a facile approach to functionalize graphene oxide with bioactive peptides, but also provides a potential biomaterial for bone repair by improving osteoblastic cell functions.

(Received April 29, 2022; Accepted September 12, 2022)

Keywords: Graphene oxide, RGD peptide, Functionalization, Biocompatibility

1. Introduction

The interactions between a biomaterial with the surrounding physiologic environment are of major relevance for determining the in vivo performance and host acceptance of any medical device [1]. Cell-material interactions including cell adhesion, proliferation, and differentiation on the material surface would occur once the devices are implanted into human body and contacted with biological tissues, and play a significant role in determining the biocompatibility of these devices. Therefore, a basic understanding of the interactions between cells and material surfaces needs to know before the application of any new implantable biomaterial.

Ever since its discovery in 2004, graphene has attracted great attention worldwide in the field of material science, owing to its remarkable physicochemical properties such as extraordinary electron transport capabilities, strong mechanical strength and excellent thermal and electrical conductivities [2-4]. These unique physicochemical properties suggest it has great potential applications in the field of electrochemistry. Recently, this versatile 2D material has expanded its territory beyond electronic and chemical applications toward biomedical are as including the promising applications in drug delivery, bioimaging, photothermal therapy and tissue engineering[5-7]. Particularly, one of the most important graphene derivatives, graphene oxide (GO), chemically exfoliated from oxidized graphite is considered as a promising materials for biological applications owing to its excellent aqueous processability, amphiphilicity, surface functionalizability and low costs [2]. Compared with pristine graphene, the abundant oxygen-

* Corresponding author: zhaochanghong@hbpu.edu.cn
# Changhong. Zhao and Xiaopei Zhang contributed equally to this work
https://doi.org/10.15251/DJNB.2022.173.989

containing groups in GO provide potential advantages for improving the bio-functionality of this nano-material by surface modification and functionalization. Even though the research regarding biomedical applications of graphene-based nanomaterials is expanding rapidly, relatively little is known about their influence on biological systems or intrinsic toxicity. It is essential to improve the biocompatibility of GO before its application into biology systems.

The Arg-Gly-Asp (RGD) sequence generally exists in the extracellular matrix (ECM) proteins and plays a subtle role in regulating the expression of integrins. Signaling molecules, such as focal adhesion kinase (FAK), Rho, protein kinase A (PKA), and extracellular signal-regulated protein kinase (ERK) driving integrin-mediated intracellular signal transduction exert a significant influence on cell functions, such as adhesion, migration, proliferation, and differentiation [8, 9]. To facilitate the cell-material interactions, RGD peptide has been immobilized to biomaterial surface to enhance the adhesion of cells to non-biological surfaces[10, 11].

Here, we conduct this study to develop a bioactive surface using RGD to functionalize GO. The immobilization of RGD peptides onto GO surface would promote cell adhesion and hence improve the biocompatibility of GO.

2. Experimental Section

2.1 Materials

Graphite powder flakes (45 μm, >99.99 wt%) are procured from Sigma Aldrich, USA. Amino acid sequence Arg-Gly-Asp (RGD, ⩾97%), 1-[Bis(dimethylamino)methylene]-1H-1,2,3-triazolo[4,5-b]pyridinium 3-oxid hexafluorophosphate (HATU, 97%) are purchased from Sigma−Aldrich (USA). $KMnO_4$, concentrated H_2SO_4, $NaNO_3$, H_2O_2, and N, N-dimethylformamide (DMF) are purchased from Aladdin (China). All chemicals were used without further purification.

2.2 Synthesis of RGD-Functionalized Graphene Oxide

The GO powder has been synthesized using the modified Hummer's method according to previously reported methods [12]. The GO (200 mg) is sonicated in 100 mL of DMF solution for 30 min at room temperature (25 °C). For the activation of carboxyl group of GO, HATU (10 mg) was added to the GO-DMF suspension under magnetic stirring for 30 min at room temperature. Then RGD (10 mg) was introduced to the above-mentioned reaction system, the reaction was kept for 1 day and 2 days respectively under magnetic stirring at room temperature. After reaction, the mixture was filtered. The filtered powder was washed with DMF thoroughly to remove the excess RGD and HATU. Finally, the obtained powder was dried for 48 h at room temperature, to get GO-RGD powder. In the following sections, the GO-RGD prepared by 1 day reaction and 2 days reaction were abbreviated as GO-RGD-1 and GO-RGD-2, respectively.

For the cell study, the as-synthesized GO-RGD powder was re-suspended into DMF, and followed by filtration in vacuum, to get GO-RGD films.

2.3 Characterizations

The composition and structure of the as-synthesized GO-RGD-2 powder have been determined by element analysis (Vario EL cube) and Fourier Transform infrared spectroscopy (FTIR, PerkinElmer Spectrum Two). The surface morphology of GO-RGD-2 film was observed using transmission electron microscope (TEM, JEOL 200CX).

2.4 Protein adsorption

Fibronectin (FN) adsorption on GO-RGD film was performed by immersing the film in FN solution (FN/PBS (10 μg mL^{-1})) for 4 h in the cell incubator. Then the films were rinsed with PBS thoroughly and immersed in 300 μL of 1% sodium dodecyl sulfate (SDS) solution for 30 min (repeated 3 times) to collect proteins adsorbed on films. The concentrations of FN were measured with an ELISA plate reader (ELx 800, BIO-TEK) and a MicroBCA protein assay kit (Pierce, Rockford, IL, USA) according to the manufacturer's manual.

2.5 Cell culture

Mouse MC3T3-E1 cells (ATCC subclone 14) were cultured in tissue culture plates containing alpha-minimal essential medium (alpha-MEM, Gibco) supplemented with 10% (v/v) fetal bovine serum (FBS, HyClone) and 1% penicillin/streptomycin (Gibco) in cell incubator at 37 °C with humidity of 95% and 5% CO_2. GO and GO-RGD films (15 mm, diameter) were sterilized in 70% alcohol solution overnight prior to in vitro study.

2.6 Immunofluorescence microscopy and cell morphology

Cells were seeded on the films at a density of ~10,000 cells per cm^2 in 24-well plates. After cultured for 24h, cells were fixed by 4% paraformaldehyde (PFA) in PBS solution for 15 min, and then permeablized in 0.2% Triton X-100 in PBS for 10 min, blocked by 1% BSA. After 30min blocking, cells were stained with rhodamine–phalloidin (Invitrogen) and 4', 6-diamidino-2-phenylindole (DAPI, Sigma). After extensive washing with PBS, cells were observed with a confocal laser scanning microscopy (ZEISS LSM 700).

Cell morphologies and spreadings on the films were also detected with scanning electron microscopy (SEM, Zeiss Supra 60 VP). After fixed with 2.5% glutaraldehyde, cells were dehydrated with gradient ethanol solution (30%, 40%, 50%, 70%, 95%, and 100%), and followed by a supercritical point drying. Finally, Cells were sputter-coated with a gold–palladium layer and observed with SEM at an accelerating voltage of 5 kV.

2.7 Cell attachment and proliferation

Cells were seeded on the films at a density of ~10,000 cells per cm2 in 24-well plates and cultured for 4 h, 1 day, 2 days, and 4 days. At each time point, cell numbers were determined by a MTT assay according to the manufacturer's protocol, and the cell attachment and proliferation represented by cell number and density.

2.8 ALP activity and calcification

After 14 days of culture in differentiation media containing α-MEM medium supplemented with 50 mg mL^{-1} ascorbic acid (Sigma-Aldrich) and 10 mM β-glycerophosphate (Sigma-Aldrich) , the ALP activity and calcium content were determined with a Fluorescence-based ALP detection kit (Sigma) and a QuantiChrom calcium assay kit (BioAssay) following the manufacturer's instruction, respectively.

2.9 Statistical analysis

Cell studies were performed in quadruplicates for each group at each time point. The statistical analysis was performed with repeated-measures two-way ANOVA using Bonferroni's post-test, and $p < 0.05$ or 0.01 in the differences between groups was considered to be significant.

3. Results and discussion

3.1 Synthesis and Characterization

As illustrated in Figure 1, GO-RGD was synthesized by amide bond formation reactions between the NH_2 group of RGD and the COOH group of GO via CO-NH. First, HATU was added to the GO-DMF suspension to yield the activated ester from the COOH group of GO, the activated ester is used for formation of amide bonds with the NH_2 group of RGD. After removed the excess RGD and HATU and dried thoroughly, GO-RGD powder was obtained.

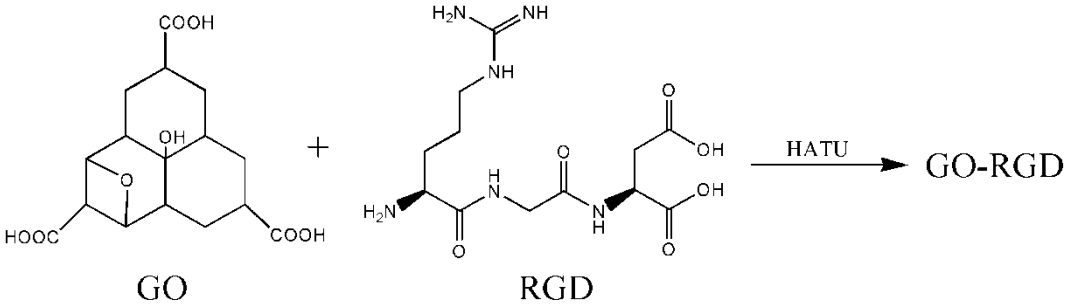

Fig. 1. Synthetic scheme of GO-RGD.

FT-IR studies have been carried out to investigate the functional groups of the synthesized GO-RGD. Figure 2 shows FT-IR spectra of the GO, RGD and GO-RGD. Comparing with GO, the peak at 1720 cm^{-1} corresponding to C=O stretching vibration of the COOH group was disappeared in GO-RGD, indicates the COOH group has been used in amide bond formation reactions, and GO was partly reduced [13]. After covalent interaction with RGD, the bands seen at 1130 cm^{-1}, 1200 cm^{-1}, and 1680 cm^{-1} in RGD spectra were also found in GO-RGD one. A dominant band observed at 1530 cm^{-1}in GO-RGD indicates the presence of amide II (60% N-H bending, 40% CN stretching) due to RGD functionalization [14]. These results reveal RGD functionalization on the GO surface.

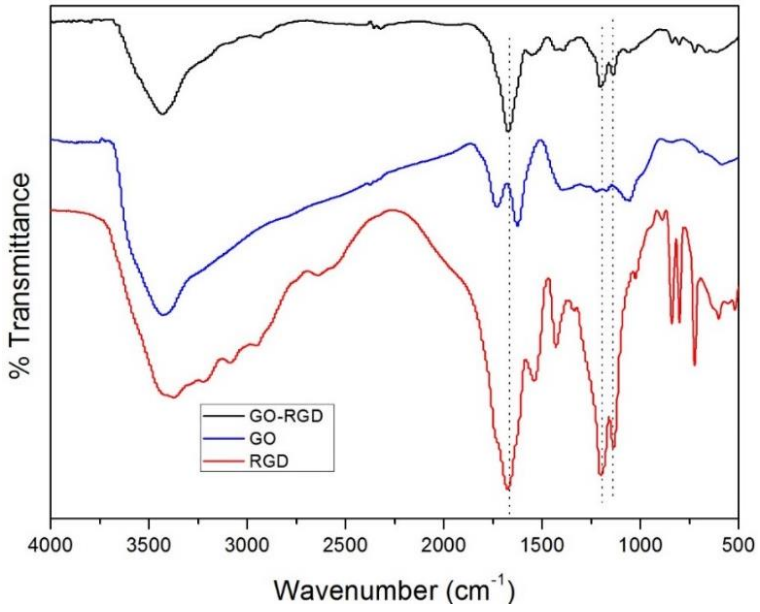

Fig. 2. FTIR spectra of GO, RGD and GO-RGD.

The chemical composition changes of the GO before and after functionalization were investigated by element analysis. As shown in table 1, compared to pristine GO, the content of C increased from 43.96% to 53.35% due to the RGD bonding. However, the O content decreased significantly from 53% to 37.9, this is probably because of the consumption of O during the amide bond formation reactions. Furthermore, the N content was almost not found in GO, but it was detected to be more than 5% in GO-RGD after coupling with RGD. These changes clearly confirmed the functionalization of GO.

Table 1. Element analysis of GO and GO-RGD.

Sample	C%	H%	O%	N%
GO	43.96	3.01	≈53	<0.3
GO-RGD	53.35	3.36	37.9	5.38

The morphologies of GO and GO-RGD were investigated using TEM (Figure 3). GO showed a typical sheet structure with wrinkles (Figure 3a). After coupling with RGD, the morpholigy has changed significantly and the colour became darker due to the reduction of GO (Figure 3b and c) [13]. The TEM image at higher magnification (Figure 3d) clearly illustrated the visually porous-like structure on the plane of GO which attributed to the successful bonding of RGD.

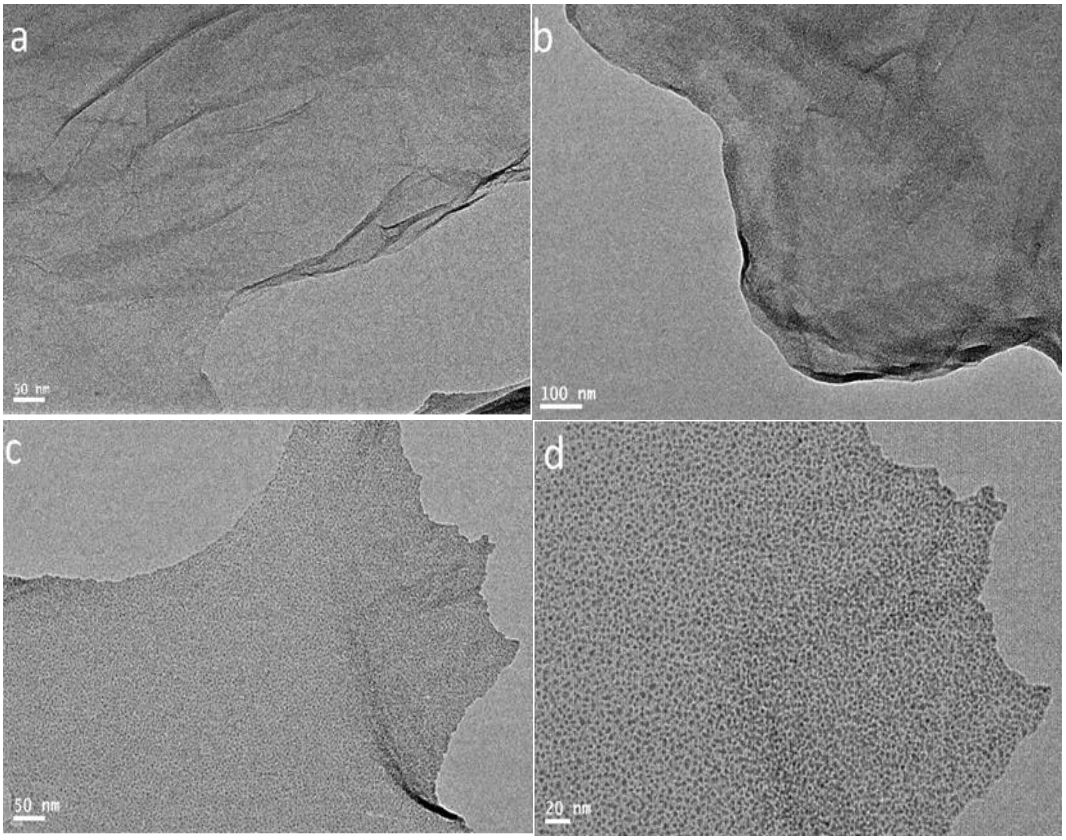

Fig. 3. TEM images of GO (a) and GO-RGD (b,c,d).

3.2. Cell adhesion

Cell adhesion was investigated with immunofluorescent staining and SEM observation as demonstrated in Figure 4. GO-RGD films showed enhanced adhesion compared with the control GO as indicated by immunostaining studies in Figure 4a. Particularly, cells on the GO-RGD-2 surface exhibited greater spreading with higher confluence than that on GO. Moderate spreading was observed on GO-RGD-1, while the cells on GO showed a more slim shape with less spreading. This finding demonstrated the enhanced cell adhesion on GO-RGD films. Cell morphologies after a 1 day culture on different films were also observed by SEM (Figure 4b). Cells on GO exhibited a poor spreading with small cell size and contacting area, whereas those on GO-RGD had a better spreading with more filopodia formed around the cellular body.

Consistently, GO-RGD-1 was observed to have a best cell adhesion with a complete spreading to the underlying surface.

Protein adsorption is the first event when materials surfaces contact biological environment and highly related to the cell responses to the materials[15, 16]. Therefore, the adsorptions of fibronectin (FN) on the GO based films were detected. The FN adsorptions were measured to be 4.5±1.1 μg cm^{-2}, 4.2±1.4 μg cm^{-2}, and 3.9±1.3 μg cm^{-2} on GO, GO-RGD-1, and GO-RGD-2 films, respectively. The FN adsorption results showed that there was no prominent difference between the GO and GO-RGD films. In the present study, the RGD peptide might play an important role in regulating cell adhesion. The signal from RGD peptide regulated the expression of integrins, for example, α_v and β_3 subunits, and the integrin-mediated intracellular signal transduction governed the cellular events including adhesion, migration, proliferation, and differentiation[17, 18]. Comparing with GO-RGD-1, GO-RGD-2 with more RGD bonding showed better cell adhesion, it suggest that MC3T3-E1 cell adhesion might be affected by the content of RGD. This also confirmed the contribution of RGD to the enhancement of cell adhesion.

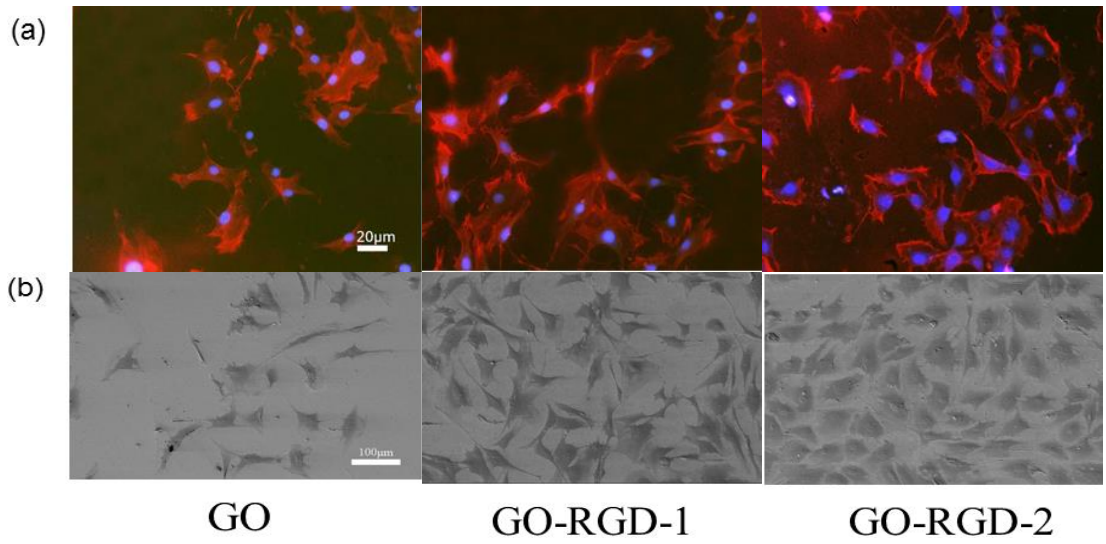

Fig. 4. Fluorescent (a, scale bar of 20 μm is applicable to all) and SEM(b, scale bar of 100 μm is applicable to all) images of cells after 1 day culture on GO and GO-RGD films.

3.3. Cell attachment and proliferation

Cell attachment at 4 h and proliferation at day 1, 2, and 4 were investigated using the CCK-8 assay. As demonstrated in Figure 5a, cell attachment measurements revealed that more cells adhered on GO-RGD films in comparison to the GO control. After 4 h culture, more than 9 $\times 10^3$ cells per cm^{-2} attached on the GO-RGD-2, which is significantly higher than that on GO-RGD-1 and GO control. The difference was smaller but still significant for GO-RGD-1 in comparison to cell attachment on GO control surface. This results suggest cell attachment was enhanced by RGD functionalized GO.

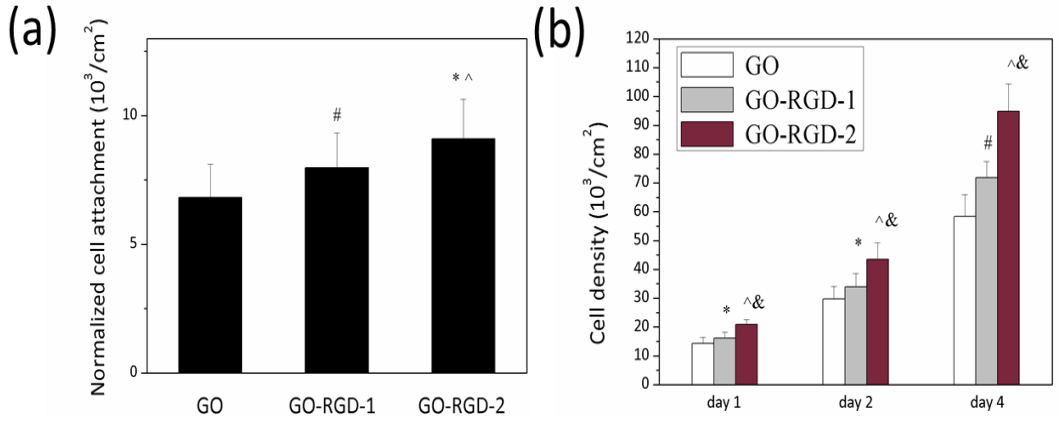

*Fig. 5. Cell attachment (a) represented by the cell numbers determined with CCK-8 assay at 4 h on the films. #: p < 0.05 relative to GO films; *: p < 0.01 relative to GO films; ^: p < 0.05 relative to GO-RGD-1 films; &: p < 0.01 relative to PLLA-d films. Cell proliferation (b) represented by the cell numbers determined with CCK-8 assay at day 1, 2, and 4. *: p < 0.05 relative to GO films; ^: p < 0.01 relative to GO films; #: p < 0.01 relative to GO films; & : p< 0.05 relative to GO-RGD-1 films.*

At each time point, the cell density was higher on GO-RGD, especially GO-RGD-2 films, than on GO films. In a good agreement with cell adhesion results, the cell proliferation on GO-RGD was significantly higher than on GO films (Figure 5b). At day 1, the cell density on GO-RGD films was remarkably higher than on GO films and the cells on GO-RGD-2 films showed the fastest proliferation. This proliferation trend became more significant when the culture time continued. As we discussed before, the enhanced cell attachment and proliferation may be attributed to the immobilization of RGD, the functional structure found in ECM proteins is able to promote cell adhesion and proliferation by interaction with integrin receptors [8].

3.4. Cell differentiation

The ALP activity and calcium content were quantified with a Fluorescence-based ALP detection kit and a QuantiChrom calcium assay kit (Figure 6).

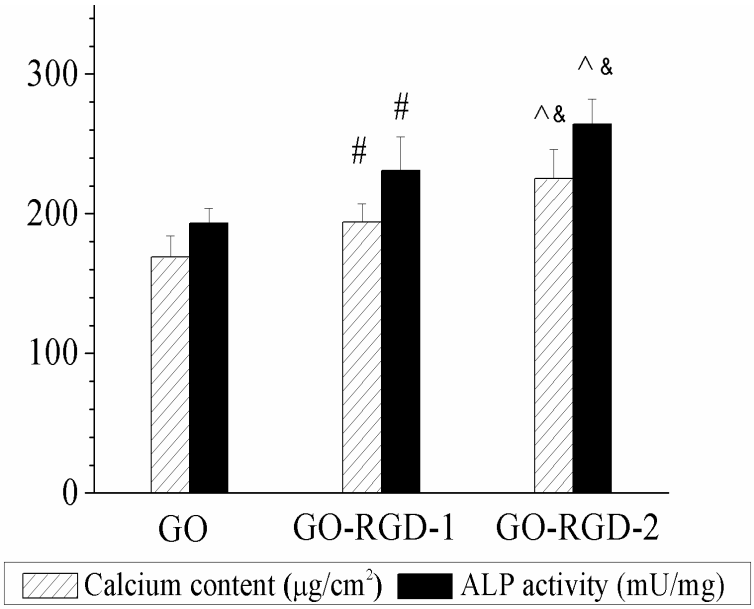

Fig. 6. ALP activity and calcium content of cells at day 14 quantified by a fluorescence-based ALP detection kit and a QuantiChrom calcium assay kit, respectively. #: p < 0.05 relative to GO films; ^: p < 0.01 relative to GO films; &: p < 0.05 relative to GO-RGD-1 films.

The intracellular ALP activity from cells on GO-RGD-2 was significantly higher than that on GO-RGD-1 and GO control. GO-RGD-1 showed a moderate level of ALP production but still higher than that of the control GO. ALP activity is regarded as an early marker of osteoblast differentiation [19], the ALP activity increased in the order of GO, GO-RGD-1 and GO-RGD-2, indicating higher differentiation level in the same order. Consistently, the calcium content in MC3T3-E1 were significantly promoted on GO-RGD films compared with GO films and the GO-RGD-2 films even induced prominently higher level of ALP activity and calcium content than GO-RGD-1films.

The enhanced differentiation of MC3T3-E1 cells on GO-RGD films might due to the better cell adhesion and proliferation. The cell confluence occurred earlier when the proliferation was faster. Consequently, the cells on GO-RGD, especially GO-RGD-2 films, reached confluence faster than GO films and subsequently the cells launched the osteogenesis earlier on GO-RGD and especially GO-RGD-2 films. In addition, previous findings indicated that nuclear expansion on special substrate surface might cause enhanced cell differentiation [20-22]. As shown in Figure 4a, the GO-RGD and especially GO-RGD-2 films showed expanded nuclei with larger area than GO films that might also contribute to the enhancement of cell differentiation on RGD functionalized GO films.

4. Conclusion

In conclusion, RGD functionalized graphene oxide (GO-RGD) was synthesized by a facile route, The immobilization of RGD on GO was confirmed by FTIR, element analysis and TEM. The RGD peptide bonding to GO promoted the MC3T3-E1 cell functions including cell adhesion, attachment, proliferation, and differentiation. Our present work might provide a potential candidate biomaterial for bone repair by improving osteoblastic cell-material interactions.

Acknowledgements

This work was supported by the Foundation of Hubei Polytechnic University (22xjz16R) and the National Science Foundation, China (Contract no. 51272153). The work on cell study was carried out within the Sustainable Production Initiative and the Production Area of Advance at Chalmers and supported by Department of Chemistry and Chemical Engineering, Physical Chemistry at Chalmers University of Technology.

References

[1] Shin, H., Biomaterials, 2007. 28(2): p. 126-133; https://doi.org/10.1016/j.biomaterials.2006.08.007

[2] Chung, C., et al., Accounts of Chemical Research, 2013. 46(10): p. 2211-2224. https://doi.org/10.1021/ar300159f

[3] Papi, M., Int J Mol Sci, 2021. 22(2); https://doi.org/10.3390/ijms22020672

[4] Gaur, M., et al., Nanotubes, Nanofibers, and Graphene. Materials (Basel), 2021. 14(20); https://doi.org/10.3390/ma14205978

[5] Grant, J.J., et al., ACS Biomater Sci Eng, 2021. 7(4): p. 1278-1301; https://doi.org/10.1021/acsbiomaterials.0c01663

[6] Prattis, I., et al., Trends Biotechnol, 2021. 39(10): p. 1065-1077; https://doi.org/10.1016/j.tibtech.2021.01.005

[7] Sattari, S., et al., Int J Nanomedicine, 2021. 16: p. 5955-5980; https://doi.org/10.2147/IJN.S249712

[8] Donahue, H.J., et al., Biomaterials, 2007. 28(10): p. 1787-1797;

https://doi.org/10.1016/j.biomaterials.2006.12.020
[9] Lagunas, A., et al., Nano Research, 2014. 7(3): p. 399-409; https://doi.org/10.1007/s12274-014-0406-2
[10] Vigneswari, S., et al., Front Bioeng Biotechnol, 2020. 8: p. 567693; https://doi.org/10.3389/fbioe.2020.567693
[11] Makowski, L., W. Olson-Sidford, and W.W. J, Viruses, 2021. 13(2); https://doi.org/10.3390/v13020146
[12] Hu, X.B., et al., Applied Surface Science, 2015. 329: p. 83-86; https://doi.org/10.1016/j.apsusc.2014.12.110
[13] An, J., et al., Materials Science & Engineering C-Materials for Biological Applications, 2013. 33(5): p. 2827-2837; https://doi.org/10.1016/j.msec.2013.03.008
[14] Liu, H.Y., et al., Nanoscale, 2014. 6(10): p. 5315-5322; https://doi.org/10.1039/c4nr00355a
[15] Lehnfeld, J., et al., J Dent Res, 2021. 100(10): p. 1047-1054; https://doi.org/10.1177/00220345211022273
[16] Cordeiro, A.L., et al., Biointerphases, 2019. 14(5): p. 051005; https://doi.org/10.1116/1.5121249
[17] Slack, R.J., et al., Nat Rev Drug Discov, 2022. 21(1): p. 60-78; https://doi.org/10.1038/s41573-021-00284-4
[18] Tjong, W.Y. and H.H. Lin, Sci Rep, 2019. 9(1): p. 1517; https://doi.org/10.1038/s41598-018-38045-w
[19] Gotoh, Y., K. Hiraiwa, and M. Nagayama, Bone and mineral, 1990. 8(3): p. 239-50; https://doi.org/10.1016/0169-6009(90)90109-S
[20] Wu, X.H. and S.F. Wang, Acs Applied Materials & Interfaces, 2012. 4(9): p. 4966-4975; https://doi.org/10.1021/am301334s
[21] Davidson, P.M., et al., Advanced Materials, 2009. 21(35): p. 3586-+; https://doi.org/10.1002/adma.200900582
[22] He, W., et al., Nat Commun, 2020. 11(1): p. 1732; https://doi.org/10.1038/s41467-020-15524-1